Track Membrane Mediated Electrostatic Introduction of Cluster Ions into TOF Mass Spectrometer

Alexander A. Balakin,† Vladimir V. Gridin, and Israel Schechter*

Department of Chemistry, Technion-Israel Institute of Technology, Haifa 32000, Israel

Received: April 21, 1998; In Final Form: September 14, 1998

Glycerol-wetted track membranes (poly(ethylene terephthalate)) are suitable for interfacing between a typical TOF chamber (held at an operational pressure of less than 10^{-6} Torr) and an ambient pressure analyte. Solute concentration aspects of track membrane mediated electrostatic introduction of negative charged species into TOF mass spectrometer were investigated. Glycerol solutions of KCl, KBr, NH_4I, and Na_2S were used. High-field charge extraction conditions were routinely maintained between the liquid samples (held at ambient pressure) and a grounded grid collector. The latter was positioned just nearby the vacuum facing side of such membranes. Upon establishing a steady-state charge extraction regime, the collector currents were monitored and recorded at various solute concentration levels. Nonlinear, solute concentration dependent, collector currents were observed and found to correspond to our theoretical treatment. Our findings are accounted for and in support of a special, evaporation limited, mechanism for the track membrane mediated high-field extraction of cluster ions.

Introduction

A large number of membrane-based vacuum inlet techniques have been recently introduced and utilized in various analytical applications of mass spectrometry.[1] To name just a few, these could be found in kinetic studies of chemical and biological reactions, analysis of environmental samples, fermentation monitoring, investigation of electrochemical processes, etc.

A pioneering usage of membrane inlets for a direct introduction of ions and their subsequent MS analysis was first reported by Yakovlev et al.[2] The resulting electromembrane ion source (EMIS) technique offers a promising potential for an on-line sampling and MS characterization of inorganic ions and even for by far larger organic entities, such as polycyclic aromatic hydrocarbons and biomolecules.

The method utilizes high electrostatic field conditions applied to a multichannel network of a submicropore track membrane (TM). TM-mediated extraction of charged species should be distinguished from the traditional methods of electrohydrodynamic ionization (EHDI).[3−5] For one, in various EMIS applications the transport of charged species, as well as the field structure, is strongly due to a dense network of a large number of quite long (10−20 μm), yet very narrow (submicrometer), channels[2,6] present in TM. Moreover, a feedback charging of the vacuum facing side of TM is of prime importance in producing high local fields.[7] This, in turn, results in the appearance of high local fields at the liquid/vacuum interface. In a steady-state extraction regime, there exists a complex interplay between the current density and the field strength there.

Despite certain advantages offered by EMIS technique for MS analysis of liquid samples, no precise mechanism of electrostatic extraction by TM is yet available. It was argued,[6] however, that any progress in EMIS-based MS analysis is pending availability of "first-hand" reliable information regarding the nature of the primary charged species extracted from liquid samples. This, in turn, requires a possibility to map and control not only the electric fields near the vacuum-facing side of the TM but also the energy distribution of the ions sent for registration inside the MS unit.

In this work, we address, for the first time, the performance of electromembrane ion sources in relation to various solute concentrations. Our target liquid samples consist of glycerol solutions of KCl, KBr, NH_4I, and Na_2S. A model of the diffusion-controlled versus evaporation-limited extraction of ionic species is introduced. We unambiguously show that in EMIS the monocharged cluster ions are by far the more preferable primary species than their multiply charged counterparts.

Experimental Section

Experimental Facility. Schematics of our experimental setup for a high electrostatic field extraction of charged species from glycerol solution are shown in Figure 1. A 10 μm thick poly(ethylene terephthalate) track membrane[6] was glued to a metal diaphragm ($d = 3$ mm) and interfaced between the vacuum and ambient pressure regions of the ion source. The typical channel density and mean channel diameter of our TM's were 10^7 cm^{-2} and 0.07 μm, respectively.

Two variable high-voltage power suppliers allowed for an independent monitoring of both ΔV (from 0 to 10 kV) and ΔW (from 0 to 3 kV). According to Figure 1, the former is set between a gold ring electrode and a fine mesh (0.2×0.2 mm^2) stainless steel grid placed at $G = 0.4 \pm 0.1$ mm from the membrane on its vacuum side. In turn, the latter is used for retarding experiments between the grid and the collector electrode. The time constant of the current readout circuit was about 1 s.

Sample Preparation. During a standard sample deposition procedure, a few (2−3) droplets of the investigated solution

* Author for correspondence. E-mail: israel@tx.technion.ac.il. Fax: +972-4-8292579.

† Permanent address: Institute of Energy Problems of Chemical Physics (Branch), Russian Academy of Sciences, Chernogolovka, Moscow Region, Russia. Research carried out at the Technion—Israel Institute of Technology.

10.1021/jp981942h CCC: $15.00 © 1998 American Chemical Society
Published on Web 10/29/1998

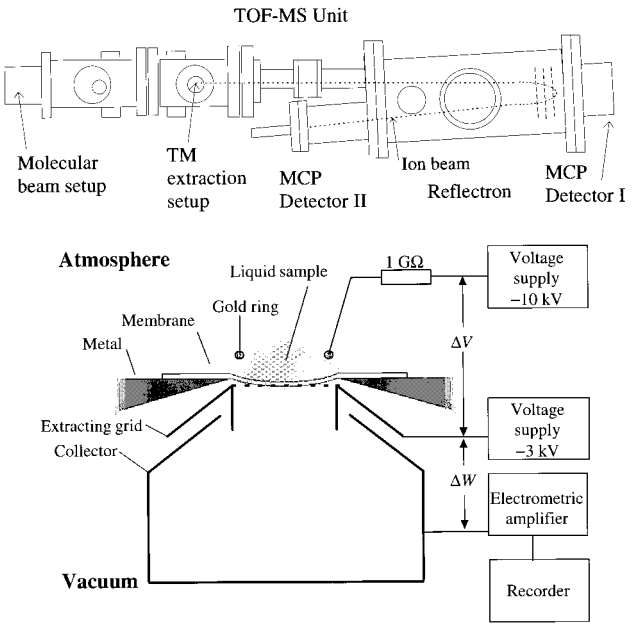

Figure 1. Schematics of the experimental setup, including the TOF-MS system (indicating the ion trajectory) (a, top) and the EMIS inlet (b, bottom). Potential drops ΔV and ΔW are used for charge extraction processes and for studying the particle/energy distribution profiles of the TM, respectively.

were placed onto the ambient pressure side of the TM. About 30 mm^2 of a glycerol-wetted area was produced. Sample renewals and/or replacements were routinely performed by a number of subsequent removal (using a blotting paper) and deposition steps. No alteration of the external voltage drop was required in any of the sample preparation procedures described.

An analytical grade glycerol (Frutarom Ltd., Israel) was used with no additional purification. Analytical grade KBr, KCl, Na_2S, and NH_4I were freshly dissolved in glycerol for preparation of the respective ionic solutions in concentration range from 10^{-6} to 0.1 M.

Results and Discussion

We first characterize the sensitivity of EMIS to both solute concentration and its ionic valent stage. The material is organized as follows: (I) description of several general features of EMIS; (II) estimation of typical field strengths involved in charge extraction; (III) transport of ions through the TM's multichannel network; and (IV) the dependence of the charge extraction upon solute characteristics.

I. General Features of EMIS. No ionization of the liquid matter is associated with neither of EHDI and EMSI related methods. Instead, in both approaches, an evaporation into vacuum occurs for those ions that are already present in the liquid phase.

In EHDI applications[3] such ion transfer is stimulated by high-field conditions, which are known to develop at the tip of a fine metallic capillary. The liquid phase is in a highly unstable state there.[5] Hence, the emission of charged species is stipulated and monitored by the instability itself.

On the contrary, only a minute disturbance of the liquid−vacuum interface is expected to occur for the various TM-based applications of EMSI technique. Indeed, in accordance with the Rayleigh stability criterion, such ionic sources could sustain (given an appropriate choice of the polymer/liquid wetting angle) quite severe electrostatic fields, i.e., of the order of 10^7 V/cm.[2,8]

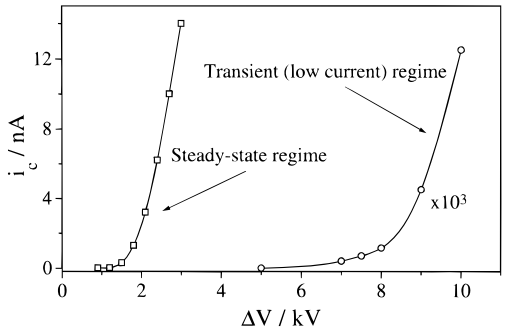

Figure 2. Typical voltage−current characteristics of the undoped glycerol solvent obtained for the transient (low current) and the steady-state operational modes of EMIS.

In electromembrane ion sources, charge extraction processes at the vacuum−liquid interface of any particular channel are subjected to an effective strength, E, of the local electrostatic field there. Clearly, in such a multichannel network as TM, only an average (per channel) field strength is assumed. For the field-stimulated evaporation of cluster ions, a single-channel contribution to the collector current, i_c, is just

$$i_c = qN_s\nu \tag{1}$$

where q is the ion charge and N_s is the number of ions present in liquid at the liquid/vacuum interface.

For such charged species, the probability of escaping to vacuum can be incorporated into the model by introducing an effective escaping frequency, ν:

$$\nu = \nu_0 \exp(-Q/kT) \tag{2}$$

Here $\nu_0 \sim 10^{14}$ s^{-1}, k is the Boltzmann constant, and T is the absolute temperature. In polar liquids, both the polarization and the evaporation energy terms should contribute to the activation energy, $Q = Q_0 - \Delta Q$. The barrier depression term ΔQ, arising from the application of the electrostatic field, is expected to follow a Schottky-type behavior,[9] namely

$$\Delta Q = q(qE)^{1/2} \tag{3}$$

Within this approach, the collector current is expected to increase as a function of increasing E and N_s. Now, using eqs 1−3 with $i_{c1} = i_{c1}(E_1)$ and $i_{c2} = i_{c2}(E_2)$, one obtains for the ratio i_{c1}/i_{c2}:

$$i_{c1}/i_{c2} = [N_s(E_1)/N_s(E_2)] \exp[(E_1^{1/2} - E_2^{1/2})/(kT/q^{3/2})] \tag{4}$$

II. Estimation of Typical Field Strength. We proceed here within the framework specified by eqs 1−4. Recall, first, that in order to initiate a nonzero current mode of EMIS,[7] a number of subsequent field busting (during about 30 s with ΔV in the range of 7−10 kV) and relaxation steps (1−2 min) are usually required. Such procedures are typically performed for about 5−10 min. They are, in fact, a clear-cut evidence[7] that a steady-state charge extraction by EMIS is preceded by a distinct transient regime.

The forthcoming estimations of E were performed for two operational modes of EMIS: the transient and the steady-state ones. In accordance with the above, an inherent characteristic of EMIS is that during a gradually evolving approach to equilibrium (i.e., throughout the transient regime) a very small charge extraction occurs at quite substantial external fields applied.[7] Our approach is separately outlined and illustrated for these cases using the data of Figure 2.

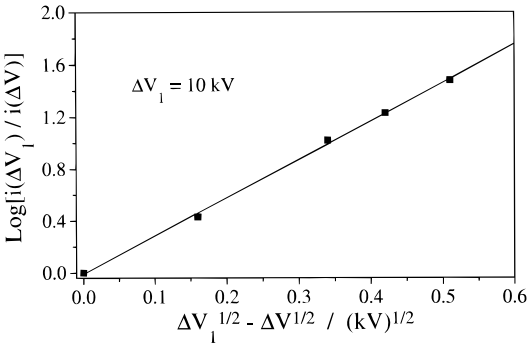

Figure 3. Plot of $\log[i_2/i_1]$ vs $\Delta V_1^{1/2} - \Delta V^{1/2}$ for the transient mode data with $\Delta V_1 = 10$ kV of Figure 2. The slope of the least mean square fit through the data provides the estimates on ξ and E; refer to eqs 5 and 6 in text.

Transient Mode of TM. In order to avoid excessive charging of the TM's vacuum-facing side, in studying the transient process, the corresponding data of Figure 2 was obtained from a low-current regime (a few picoamperes) by repetition of several short-time applications of ΔV. Had ΔV been kept on for longer than ~30 s, a current-bursting mode could have been developed. This, in turn, could become so intense that a number of fine glycerol droplets would have formed at the vacuum side of the TM (i.e., with high chances of touching the grid and short-circuiting the EMIS).

In the low-current case of the transient operational regime (refer to Figure 2), any substantial contribution to E from the surface charge density, σ, could be neglected. Moreover, on a similar footing, we assume that for the 7 kV $\leq \Delta V \leq$ 10 kV interval N_e is independent of E too. Hence, under such circumstances we may write

$$E = \xi \Delta V/G \tag{5}$$

where ξ is a unitless geometrical factor. It is expected to vary from one TM to another due to a random variation in the mean channels' diameter and their surface density.

Using eq 5 for E of eq 4 we obtain

$$i_c(\Delta V_1)/i_c(\Delta V_2) = \exp[(\xi q^3/G)^{1/2}(\Delta V_1^{1/2} - \Delta V_2^{1/2})/(kT)] \tag{6}$$

Now, while fixing $\Delta V_1 = 10$ kV and varying $\Delta V = \Delta V_2$ in eq 6, the value of ξ is readily obtained. This is demonstrated in Figure 3, where we use semilogarithmic axes to plot the left-hand side of eq 6 versus $(\Delta V_1^{1/2} - \Delta V^{1/2})$.

At room temperature, the slope of this plot ($\cong 3$ kV$^{-1/2}$) yields $\xi \approx 7$. Using this value in eq 5 we find $E_1 \approx 1.4 \times 10^6$ V/cm for $\Delta V_1 = 10$ kV. This field strength for a low-current regime, however, is in excess of an order of magnitude lower than its electrostatic estimate for a needlelike channel geometry case.[6]

Such a discrepancy in the various estimates might be due to the in-plane surface charge transfer at the vacuum-facing side of the TM. This possibility is experimentally substantiated by the data of Figure 4. Indeed, the surface charge relaxation effects are those responsible for a fast (a few seconds long only) decay of E (evidenced by that of i_c there) from the instant at which ΔV was brought to nil. Next, let us estimate the electric field strength in a steady-state regime.

Steady-State Mode of TM. At a several-nanoampere level of i_c, the steady-state regime is readily entered in by simply reducing ΔV to a usual operational mode with ΔV in a 0.3−3 kV range. The current−voltage dependence in this steady-state region is shown in Figure 2 too. For this mode N_s is

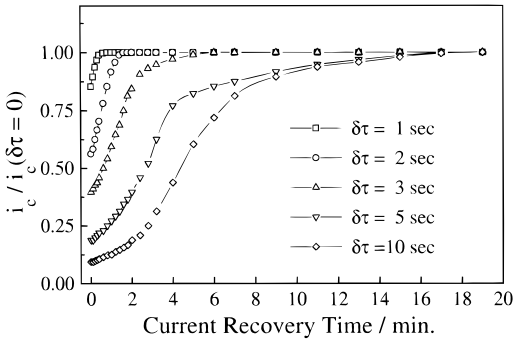

Figure 4. Typical current recovery kinetic measurements performed at $\Delta V_1 = 10$ kV inside the transient regime. Different sets of data correspond to the short time periods during which the potential drop was forced to nil: 1 s, 2 s, 3, 5, and 10 s. Observe a quick falloff of i_c (and the associated E) for the quite minute disturbances of the charge-extracting conditions in this regime. Such behavior is indicative of an insignificant surface charge density.

proportional to E. Hence, in terms of eq 4 we find

$$i_{c2}/i_{c1} = (E_2/E_1)\exp[(E_2^{1/2} - E_1^{1/2})/(kT/q^{3/2})] \tag{7}$$

Substituting $X \equiv (E_2/E_1)^{1/2}$ we get from eq 7

$$X = 1 + (kT/q^{3/2}E_1^{1/2})\ln[(i_2/i_1)/X^2] \tag{8}$$

We now consider the low-current portion of the steady-state regime data of Figure 2. For this case, i_{c1} is comparable to that obtained for $\Delta V = 10$ kV in the transient regime mode of the TM. Hence, we make a simplifying substitution in eq 8 and let $E_{c1} = 1.4 \times 10^6$ V/cm there too. This way, with i_{c2} being measured at $\Delta V = 3$ kV of the steady-state mode, we obtain $i_{c2}/i_{c1} \cong 10^3$. Hence $X \cong 1.4$ solves eq 8 and leads to $E_2 \cong 2.7 \cdot 10^6$ V/cm. This value is by far larger than $\Delta V/G = 6 \times 10^4$ V/cm. It was recently argued[7] that such high fields result from charging the TM's vacuum-facing side by the positive ions generated on the extracting grid when the current is large enough. Since neither the geometry of the surface charge nor the working surface of the channel is specified, the above estimates provide an effective order of magnitude for E only.

As a closing remark for this subsection, we note that a cluster-ion like structure, rather than a charged-droplet structure, of the liquid escaping material was assumed. Experimental evidence in support of such an assumption will be provided in the following subsection. Labeling the valence stage of a single ion by w, the form that specifies these cluster ions is $A^{-w}(\text{glycerol})_m$. According to this notation, they are composed of m solvent molecules attached to either the deprotonated glycerol molecules or the ions released upon dissociation of the respective salts. For the latter case A = I, Cl, Br ($w = 1$), or S ($w = 2$).

III. Transport of Ions. Field-mediated transport of charge carriers is of a prime importance for EMIS. Naturally, prior to dealing with ionic motion down the multichannel network of track membranes, we present our electroconductivity data obtained on bulk samples.

Electroconductivity of Bulk Samples. The specific conductivity, γ, of ionic solutions is given by

$$\gamma = q_- n_- \mu_- + q_+ n_+ \mu_+ \tag{9}$$

where q, n, and μ stand, respectively, for the charge, carrier

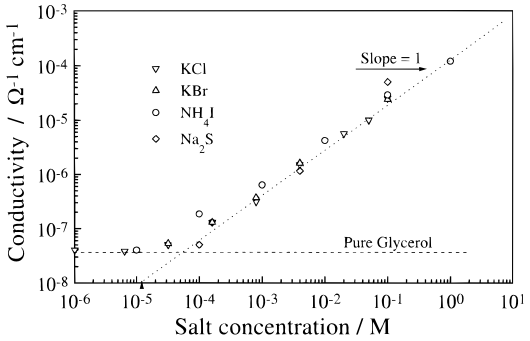

Figure 5. Electroconductivity of bulk samples as a function of the majority carrier concentration, *C*, for the solutions studied. Electroconductivity was measured in a standard potentiometric cell (two plane electrodes of 1 cm^2 each placed at 1 mm gap apart).

density (cm^{-3}) and mobility of the ions; the subscripts + (−) correspond to the positive (negative) species present.

Assuming $n_- = n_+ \approx 10^{-3}N_AC$, where N_A is Avogadro's number and C is the molar salt concentration, one obtains $\gamma \sim C$. This relation is in accordance with the data of Figure 5 (i.e., the slope = 1). The data also suggest that for the ionic solutions studied, $\mu^* \equiv (1/2)[\mu_+ + \mu_-] = 2 \times 10^{-6}$ cm^2/(V•s) and is virtually solute type independent. In turn, with this estimate of μ^* and by means of eq 9, we find that, for the analytical grade glycerol used, the molar concentration of deprotonated glycerol molecules is of the order of 10^{-6} M (or 5×10^{14} cm^{-3}).

TM-Mediated Charge Transport. A multichannel network of TM imposes severe restrictions on ionic transport in glycerol solutions. There are two interrelated mechanisms involved: (1) a diffusive supply of ions toward the vacuum/liquid interface and (2) a high-field-mediated evaporation of ionic species to the vacuum region. Let us elaborate on this next.

An application of ΔV results in charge redistribution inside the multichannel network. In particular, a buildup of the space-charge layer takes place. The larger the bulk carrier density, n, the narrower such a layer would be. Its corresponding thickness, measured from the liquid−vacuum interface, could be approximated by means of the, so-called, Debye length, L_D:

$$L_D = (\epsilon kT/8\pi nq^2)^{1/2} \qquad (10)$$

where ϵ is the static dielectric constant of the solution (=42 for pure glycerol). The effect of such space charge is to shield the extracting field, E. In what follows, n_0 and Δn stand for the background carrier densities of solvent and solute, respectively; also $n = n_0 + \Delta n$.

Let x be an axial distance inside the channel, so that $x = 0$ at the liquid/vacuum interface. Hence, at a certain $x \gg L_D$, we expect $E = 0$. Using eq 10 for pure glycerol, one obtains $L_D \leq 200$ nm for $n \geq 5 \times 10^{14}$ cm^{-3}. Note that the channel length, $l \approx 10^{-3}$ cm, is significantly larger than L_D for all the ionic concentrations used. In a sense, L_D provides a relevant length scale for estimating the extent of E inside the liquid phase. Since the current in our study was low enough, high local fields act in the channels in the vicinity of the liquid−vacuum interface only.

In turn, a corresponding length scale for E on the vacuum side of the TM could be found as follows. In accordance with the above, the potential drop in the liquid phase is about EL_D (≈10 V). On the other hand, the loss of kinetic energy was measured by retarding experiments and is presented in Figure 6. It is referred there as $\delta\epsilon$ (≈100−300 eV) and cannot be accounted for by EL_D alone.

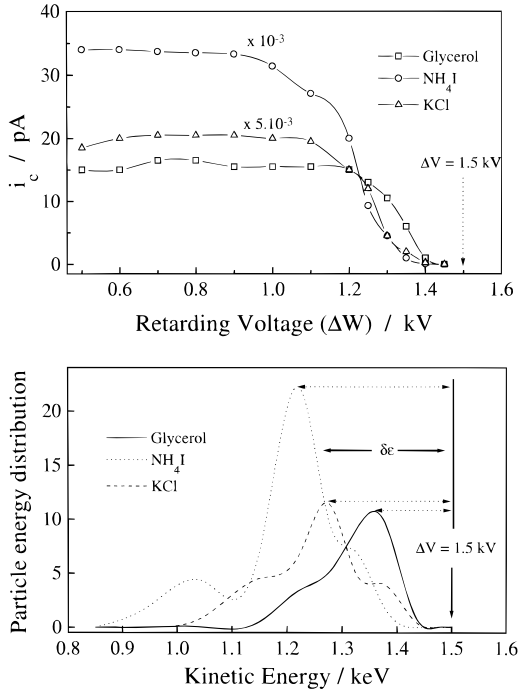

Figure 6. (a, top) Results of typical retarding experiments performed in a steady-state extraction regime: here the stopping potential, ΔW, was varied within {0; 1.5 kV} interval, while the applied ΔV was adjusted to keep the potential drop (between the liquid sample and the grid) constant and equal to 1.5 kV. (b, bottom) Particle density vs kinetic energy plot obtained as a numerical derivative of the spectra in (a). Observe an increase of the energy loss, $\delta\epsilon$, as a function of increasing i_c. On a qualitative footing, this observation is in accordance with an enhanced feedback accumulation of the surface charge, which is needed to create and maintain high electrostatic fields at the liquid/vacuum interface.

Such losses might result, however, from a high-field-mediated decomposition of the cluster ions on the vacuum side of the TM, nearby the interface region. If so, then an effective extent of E into the vacuum half space could be estimated too. Indeed, let M be a mass of a primary cluster ion, whereas, upon decomposition, it becomes M_1. Hence, the distance, Δ, where such decomposition takes place is estimated by $M_1\epsilon_1/MqE$. This leads to $\Delta \approx 10^{-5}-10^{-4}$ cm even for $M_1/M \approx 1$. Having established an effective range of influence for E, we proceed treating ionic transport inside the TM.

Let x^* be such that: $l \gg x^* \gg L_D$. Define n^* to stand for the mean carrier concentration inside the $\{x^*, 0\}$ interval. In accordance with the above, the corresponding field strength at x^* would nearly vanish, producing, thus, a nearly field-free region there. On the other hand, due to the charge extraction processes at the liquid−vacuum interface, one might expect $n^* < n$.

Hence, in order to maintain dynamic charge extraction, a diffusive charge carrier transfer should set in. Let $D = kT\mu/q$ and S_c stand, respectively, for the diffusion coefficient and the mean cross section of a single channel. Recalling eq 1 for i_c we also write

$$i_c = qDS_c(n - n^*)/l \qquad (11)$$

This, in fact, conditions the very existence of the charge extraction processes by the concentration gradient dependent driving force. The number of ions on the liquid−vacuum

interface can be approximated by

$$N_s \approx \sigma S_c \delta / qL_D \tag{12}$$

where σ is the surface charge density (defined by $E = 4\pi\sigma$), δ is the thickness of the liquid surface from which the ions can transfer into vacuum. Defining $i_{cm} = qDS_c n/l$ and $i_{c0} = qDS_c n_0/l$, and using eq 11, one obtains $n^*/n = 1 - i_c/i_{cm}$. When dealing with solutions (as opposite to the pure glycerol case), an average escape frequency, ν_{av}, should be used (it will be explicitly introduced in the forthcoming paragraph). Hence, according to eq 1, $i_c = qN_s\nu_{av}$. Now, while applying eq 12 and upon substituting n^* for n of L_D (refer to eq 10), we arrive at

$$i_c = qS_c\delta\nu_{av}E[n(1 - i_c/i_{cm})/(2\pi\epsilon kT)]^{1/2} \tag{13}$$

which specifies $i_c = i_c(n)$. With $Y = (n_0/n)(i_c/i_0) = i_c/i_{cm}$ and $B = \delta\nu_{av}lE/D(2\pi\epsilon kTn)^{1/2}$, eq 13 gives

$$Y^2 = (1 - Y)B^2 \tag{14}$$

while the physically sound solution of it is

$$Y = [(1 + 4/B^2)^{1/2} - 1](B^2/2) \tag{15}$$

IV. Solute-Dependent Extraction. Consider now two limiting steady-state situations for the charge extraction functioning of track membranes, when $n \neq n_0$.

First Case: $Y \rightarrow 1$ for $B \rightarrow \infty$. The *diffusion-limited* (or an *instant evaporation)* regime results (for $\Delta n \gg n_0$), in accordance with eq 15, in

$$i_c \rightarrow i_{cm} \sim \Delta n; \quad \text{for } B = \delta\nu_{av}lE/D(2\pi\epsilon kTn)^{1/2} \rightarrow \infty \tag{16a}$$

Hence, an instant evaporation would require a full-scale, diffusive supply of the charge carriers involved. It results in a linear dependence of i_c on Δn while the charge extraction functioning of track membranes is limited by the diffusive transfer of the carriers down the multichannel network. For $C = 0.1$ M a rough estimate provides $i_{cm} \approx 10-100$ nA (when about 10^6 channels are active in a process).

Second Case: $Y \rightarrow B$ for $B^{1-} \rightarrow \infty$. The *evaporation-limited* (or an *instant-diffusion*) regime is also derived from eq 15 and results (for $\Delta n \gg n_0$) in a square-root variation of i_c with Δn, namely:

$$i_c \rightarrow i_{cm}B \sim \Delta n^{1/2}; \quad \text{for } B^{-1} = D(2\pi\epsilon kTn)^{1/2}/\delta\nu_{av}\, lE \rightarrow \infty \tag{16b}$$

This situation occurs whenever the carriers' supply toward the liquid−vacuum interface is by far more efficient than their field mediated evaporation into vacuum.

Multiple Carrier Extraction. The above derivations, leading to eqs 16, actually assumed a single type of majority carriers. No attempt was made, so far, to address a possibility of $\nu = \nu(n)$. Such simplifications are, in part, substantiated by our conclusions drawn in regard to the experimentally obtained mobilities of the various glycerol solutions. In any real case, however, a high-field-mediated charge evaporation process might occur with more than one type of ionic solutes. Here we consider a straightforward, double carrier case, which could be readily generalized to a more complex one.

Let Δn_1 and Δn_2 specify, respectively, majority carrier densities of two distinct ionic species present in a glycerol solution (including the deprotonated glycerol). As before, $n_1 = n_0 + \Delta n_1$ and $n_2 = n_0 + \Delta n_2$. Prior to mixing, the associated

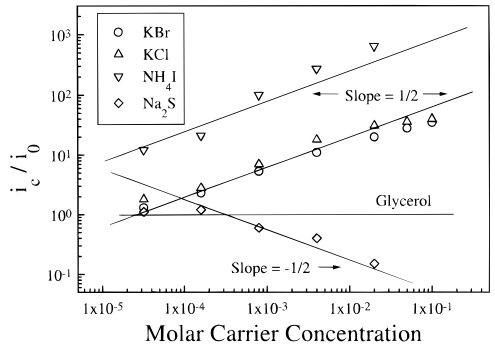

Figure 7. Typical solute type and concentration dependent plots of i_c/i_0 measured at $\Delta V = 1.0$ kV.

charge extraction processes from the respective solutions are characterized by the escape frequencies ν_1 and ν_2. Hence, the mean escape frequency is set equal to

$$\nu_{av} = (n_1\nu_1 + n_2\nu_2)/(n_1 + n_2) \tag{17}$$

[Note: The notation used at various steps leading to eqs 16, for example, $n_1 = n_0$, $n_2 = n_0 + \Delta n$, $\nu_0 = \nu_2 = \nu$; hence, with $\Delta n \gg n_0$, eq 17 provides $\nu_{av} \approx \nu$ as before.]

On the base of eq 17, a number of peculiar features found in our experimental data will be satisfactory accounted for. Recall that $n_0 \approx 10^{-6}$ M for the glycerol solvent itself; therefore, slightly more generally, with $n_1 = n_0 \ll n_2 = n_0 + \Delta n$, there are two limiting situations to be considered: (a) $n_1\nu_1 \ll n_2\nu_2$ and (b) $n_1\nu_1 \gg n_2\nu_2$. They lead for the former and latter cases, respectively, to

$$\nu_{av} \approx \nu_2, \quad \text{i.e., is effectively independent of } \Delta n \tag{17a}$$

$$\nu_{av} \approx \nu_2/n_2, \quad \text{i.e., is proportional to } 1/\Delta n \tag{17b}$$

Comparison with Experimental Data. Our results for the salt concentration dependent evaporation of charged species are shown in Figure 7. Such clear-cut dependence of i_c on the type and nature of ionic solutes unambiguously justifies our concept of evaporation of cluster ions by EMIS. On a qualitative footing, these findings are in favor of a crucial role played by polarization effects in EMIS. Indeed, the larger the ion radius, r, is, the smaller should the associated polarization energy term be. Hence, in accordance with recent MS observations,[6] a number of the solvent neutrals (extracted with a single halogen ion) decreases with increasing r. Therefore, a further enhancement of the escape frequency, ν, should then result.

Such trend, clearly, would imply an effective growth of i_c when larger halogen ions are used. This behavior is also illustrated in Figure 7. We note, however, that a slight increase of i_c (inspect KCl and KBr data) does not match the expectations based on the ionic radii considerations alone. It seems likely that the sizes of the cluster ions escaping the liquid would not be as different as the corresponding radii of the halogen ions are. Because of this, the electrical part of the energy barrier on the liquid−vacuum interface levels off and brings about only a minute variation of i_c.

Having in mind all this, we maintain that the divalent cluster ions should be composed of a larger number of glycerol neutrals than their monovalent counterparts. Hence, the corresponding activation barrier for S^{2-} is expected to be enhanced. Due to the associated reduction of ν, a poorer charge extraction performance of the TM should be anticipated.

Inspecting Figure 7 for all the monovalent ions studied, the observations are in favor of the evaporation-limited regime. In

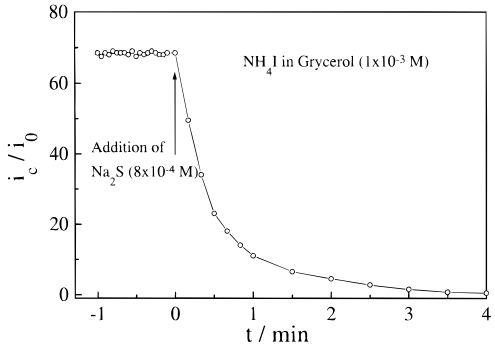

Figure 8. Collapse of the steady-state charge extraction regime of a monovalent 1×10^{-3} MNH_4I/glycerol sample upon introduction of a small (3:1 by volume ratio) amount of a divalent 8×10^{-4} M Na_2S/glycerol sample. Such behavior is in accordance with eqs 16b and 17.

other words, it is being specified by eq 16b in conjunction with a solute type dependent conditioning of eq 17a. Indeed, the slope of 1/2 is evidenced for these cases.

On the other hand, an increasing concentration of the divalent ions (contributed by Na_2S) has produced a decreasing tendency, $i_c/i_0 \sim \Delta n^{-1/2}$, with an effective slope of $-1/2$ in this figure. Clearly, this should correspond to the behavior governed by eqs 16b and 17b. Additional substantiation of our model is evident from Figure 8. There, in accordance with eq 17, a quite dramatic reduction of i_c is caused by a minute deposition of S^{2-} ions. We note in this regard that, provided that at high enough solute concentration the multiply charged species would be forced to appear at the liquid−vacuum interface, a similar falloff of i_c could be anticipated for a monovalent salt too. Indeed, a significant decay of i_c was observed by us for KCl and KBr glycerol solutions with $\Delta n \geq 0.02$ M.

Conclusions

Charge extraction processes by means of a high-field-evaporated charged droplets (as in EHDI) is primarily governed by various *macroscopic* properties of the liquid phase. These include the viscosity, electrical conductivity, surface tension, etc. In each case, the *microscopic* parameters of the majority carriers are less important. Here, however, it was rigorously demonstrated, both theoretically and experimentally, that the extraction efficiency of EMIS is strongly influenced by the ionic radii, valence status, and concentration of the majority carriers present in the liquid phase. We, hence, provide for the first time, a clear-cut evidence in favor of a cluster ion structure, rather than a charged-droplet like structure, of the liquid escaping material species in EMIS. Our findings bring one step further the possibility to develop an essential "know-how" for interfacing EMIS to the TOF-equipped mass spectrometric analyzers.

Acknowledgment. This research was supported by the Israel Ministry of the Environment, by the James Franck Program for Laser-Matter Interaction, by the Israel Science Foundation, and by Grant 95-03-09083 of the Russian Foundation for Basic Research. We thank L. I. Novikova for preparing and testing the membranes used in this research.

References and Notes

(1) Lauritsen, F. R.; Kotiaho, T. *Rev. Anal. Chem.* **1996**, *15*, 237−264 and references therein.

(2) Yakovlev, B. S.; Talrose, V. L.; Fenselau, C. *Anal. Chem.* **1994**, *66*, 1704−1707.

(3) Stimpton, B. P.; Evans, Jr., C. A. *J. Electrost.* **1978**, *5*, 123−144.

(4) Cook, K. D. *Mass Spectrom. Rev.* **1986**, 467−519.

(5) Dülcks, T.; Röllgen, F. N. *Int. J. Mass Spectrom.* **1995**, *148*, 123−144.

(6) Balakin, A. A.; Dodonov, A. F.; Novikova, L. I.; Talrose, V. L. *Rapid Commun. Mass Spectrom.* **1996**, *10*, 515−520.

(7) Balakin, A. A.; Dodonov, A. F.; Novikova, L. I.; Talrose, V. L. *J. Electrost.* **1997**, **40&41**, 615−620.

(8) Yakovlev. B. S. *High Energy Chem.* **1995**, *29*, 389.

(9) Condon, E. U., Odishaw, H., Eds. *Handbook of Physics*; McGraw-Hill: New York, 1958; Chapter 8.